Supporting Information

Growth dynamics and electron reflectivity in ultrathin films of chiral heptahelicene on metal (100) surfaces studied by spin-polarized low energy electron microscopy

Miloš Baljozović, André L. Fernandes Cauduro, Johannes Seibel, Anaïs Mairena, Stéphane Grass, Jérôme Lacour, Andreas K. Schmid, Karl-Heinz Ernst

Table of content

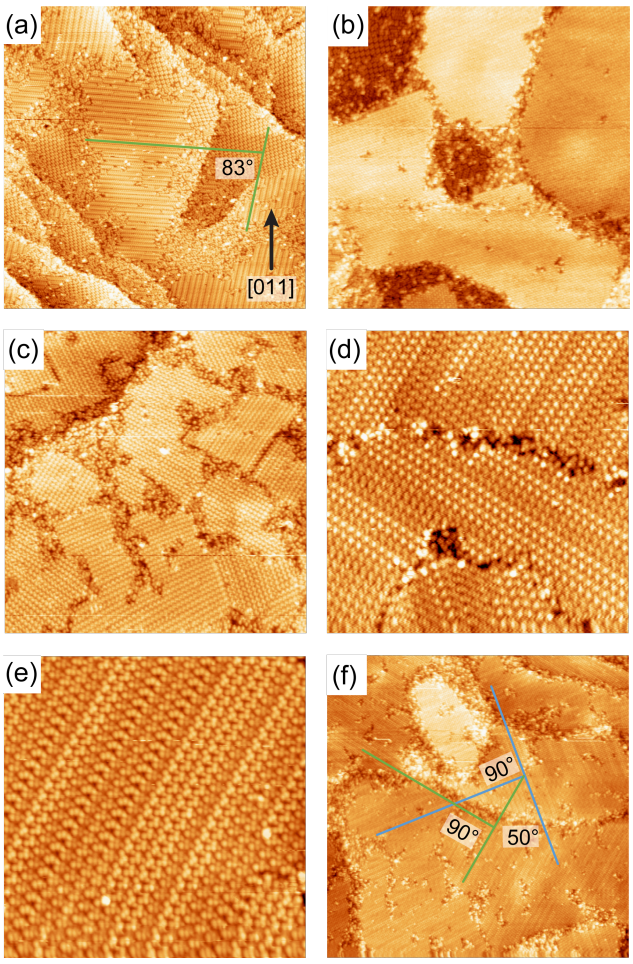

Figure S1. STM images at coverages beyond one monolayer. a) overview STM image (150 nm × 150 nm, $U = 2.05$ V, $I = 51$ pA) of *M*-[7]H at the coverage where formation of the second layer starts. The first layer shows a quadruplet structure. A structure with molecules partly in the first layer and with rows of molecules in the second layer shows mirror domains aligned at 83° to each other. b) Overview STM image (133 nm × 133 nm, $U = -2.73$ V, $I = 22$ pA) of *(M)*-[7]H with formation of compact second layer islands. Darker parts represent the first layer. c) STM image (80 nm × 80 nm, $U = -2.73$ V, $I = 46$ pA) of *rac*-[7]H at the coverage where transformation to row structure occurs. The ordered row structure is surrounded with disordered 1st layer molecules due to molecular depletion. d) STM image (40 nm × 40 nm, $U = -2.73$ V, $I = 24$ pA) of a compact 2nd layer of *rac*-[7]H with row-like appearance. e) STM image (30 nm × 30 nm, $U = -2.67$ V, $I = 35$ pA) with submolecular resolution of the 2nd layer of *rac*-[7]H. Homochiral rows of both enantiomers are observed. f) Overview STM image (200 nm × 200 nm, $U = 2.84$ V, $I = 24$ pA) of 2nd layer *rac*-[7]H layer structure showing the relative orientation of rotational (90°) and mirror domains (50°).

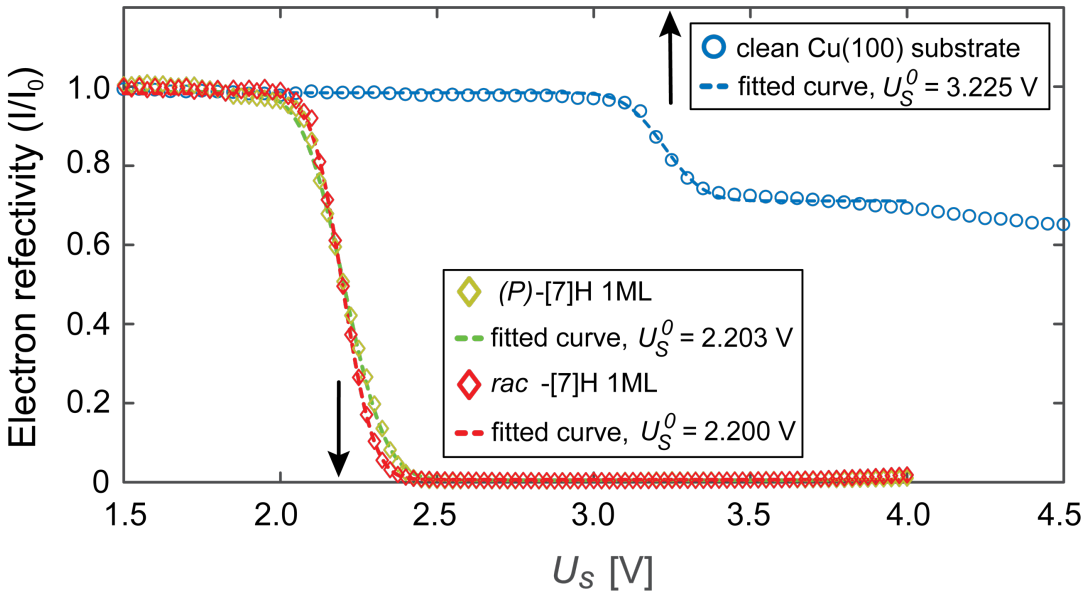

Figure S2. LEEM I-V spectra of clean Cu(100) (blue circles), 1 ML *(P)*-[7]H (green diamonds) and 1 ML *rac*-[7]H (red diamonds) on Cu(100) as well as their fitting (dashed colored lines). Black arrows indicate the value of the work function obtained from the turning point of the curves.

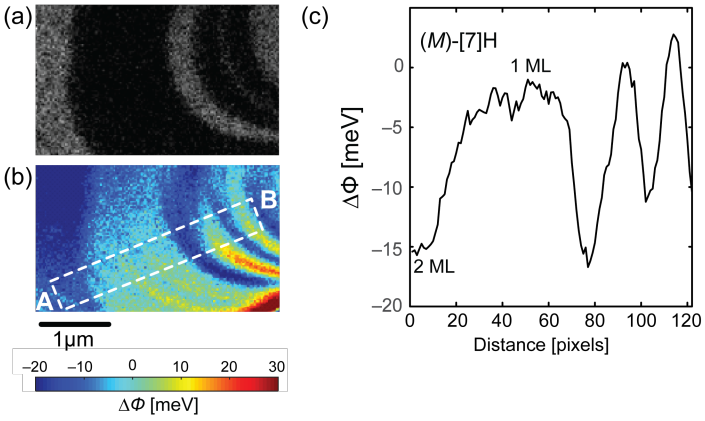

Figure S3. LEEM image and 2D work function differences map ($\Delta\Phi$ [eV] = $\Phi - \Phi_{dark}$) and line profile. a) LEEM bright field image (U_S = 3.2 V) of (*M*)-[7]H showing 2 ML tiles (bright) and 1st layer (dark). b) Pixel-by-pixel work function map of the surface shown in (a) exhibiting work function contrast between 1 ML and 2 ML regions. A gradient from the left upper corner to the lower right corner is an artifact due to non-uniform illumination of the electron beam. The line profile is affected insignificantly as it is taken in a direction perpendicular to this artifact gradient. c) Line profile revealing that the 2 ML thick film of (*M*)-[7]H has also a 15 ± 5 meV lower work function with respect to the 1 ML (*P*)-[7]H.

Comment on origin of gradient

The design of the low energy electron microscope used in this work is optimized for applications using a spin polarized electron beam. For optimal stability of the orientation of the spin

polarization, the magnetic beam separator used here implements a compensated set of dipole magnets, so that the beam separator does not rotate the electron spin polarization. Astigmatic focusing properties of these dipole magnets are then compensated by electrostatic cylinder lenses so that, under perfect alignment conditions, the direction of electron trajectories throughout the entire field of view of 12 μm is normal to the sample surface (for a detailed description of the design see Ref. [K. Grzelakowski, and E. Bauer, A flange-on type low energy electron microscope, Review of Scientific Instruments 67, 742 (1996); https://doi.org/10.1063/1.1146802]). In reality, this condition cannot be achieved perfectly: perfectly normal electron trajectory incidence across a finite field of view would imply that the brightness of the electron source is infinite. In reality, during daily operation of this SPLEEM slight drifts of alignment conditions occur, e.g. as a result of room temperature drift. One resulting condition can be that the direction of electron trajectories becomes slightly position-dependent. This effect is particularly visible in work function maps, which are essentially maps of the voltage applied between the sample and the spin polarized photocathode at which the normal component of the electron energy in each image pixel vanishes. In conditions of perfect alignment, this voltage is equal to the work function difference between the two. In the image reproduced in Figure S3, alignment is slightly off: the direction of electron trajectories gradually changes from essentially perfect alignment with the surface normal in the upper left part of the image to slightly tilted away from the surface normal in the lower right. As discussed in the detailed analysis by Jobst et al. [Ref 41, J. Jobst, L. M. Boers, C. Yin, J. Aarts, R. M. Tromp, S. J. van der Molen, Ultramicroscopy 2019, 200, 43.] trajectory tilt leads to an offset of the apparent work function. However, because this trajectory tilt varies very gradually and because our measurement profile was selected orthogonal to the artifact trajectory tilt gradient, this gradual offset cancels in our measurement of work function differences between nearby 1st layer and 2nd layer regions and it is negligible within the error bar of this measurement of ± 5 meV.

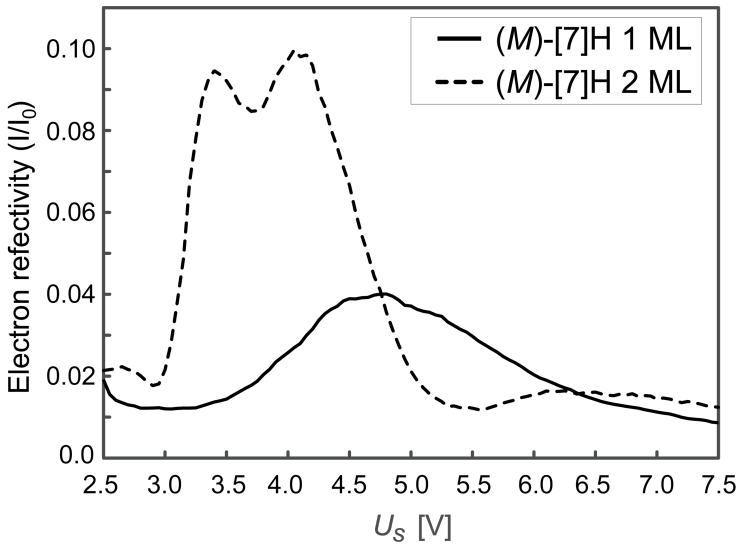

Figure S4. LEEM electron reflectivity *versus* start voltage plots of 1 ML (solid black line) and 2 ML (dashed black line) thick layers of *(M)*-[7]H on Cu(100) substrate. Shapes and intensities of the curves are similar to the ones shown for *(P)*-[7]H on Cu(100) in Figure 4.

Racemic

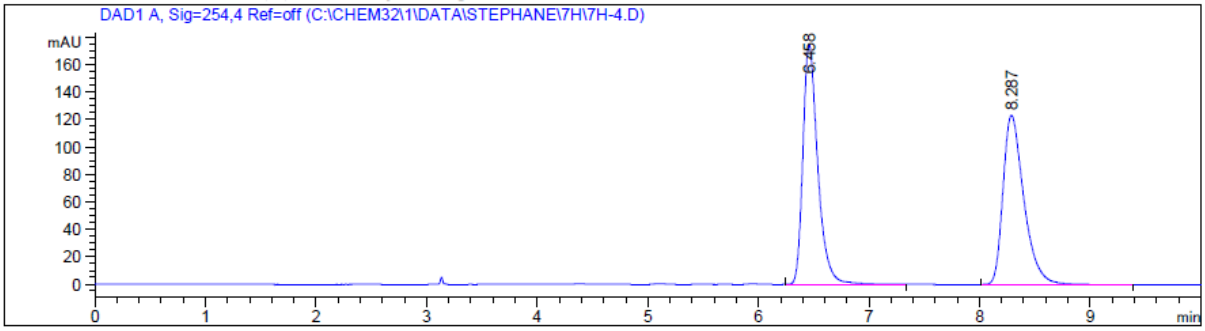

First eluted enantiomer, *ee* > 99.9%

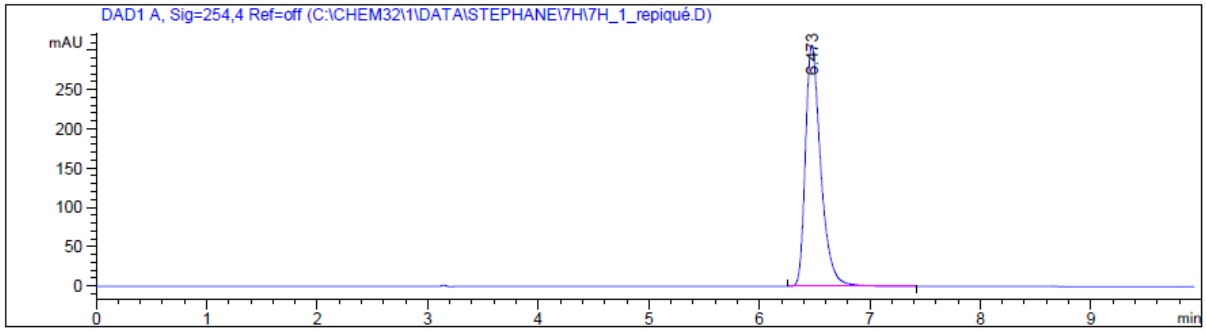

Second eluted enantiomer, *ee* > 99.9%

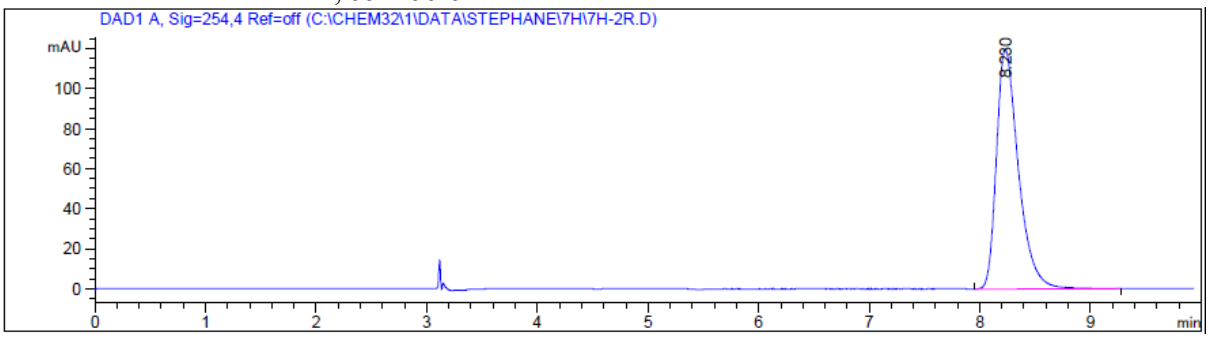

Figure S5: HPLC analyses of racemic and pure enantiomers showing an enantiopurity of more than 99.9% for each of the separated enantiomers.